4th National & 2nd International Conference on Applied Research in
Electrical, Mechanical and Mechatronics Engineering
February 2017 Tehran, Iran

Intelligently Tuned μ-PID for Aircraft Lateral Control

H. Panahi – S. Seyedtabaii
Elec. Eng. Dept., Shahed Univ., Tehran, IRAN

ABSTRACT

Aircraft control is often exposed to disturbances and uncertainties. Accomplishing safe and secure flight requires robust controls. The well-known robust methods usually suggest large in size controllers. In this paper, a PID sized controller (μ-PID) is designed where both the robust frequency domain merits, observed by the robust techniques, and the time domain desires contribute. The performance index weights are appropriately set to match the intended goals. The optimization process is conducted using particle swarm optimization (PSO) technique. The H_∞, μ synthesis and the μ-PID designs are used for a multi-input multi-output (MIMO) flight lateral control. The controlled variables are the roll angle ϕ and the sideslip angle β. The numerical simulation demonstrates that the proposed method with lower sized controller can yield performances better than what the robust methods such as the H_∞, μ synthesis designs succeed.

Keywords: Robust controller, Mu-PID, Aircraft lateral system, Parametric uncertainty, Disturbance rejection.

1 INTRODUCTION

Any control law should enforce precise control in the face of nonlinearities, disturbances and uncertainties. Conventionally, the system is linearized around an operating point and a controller is designed to fulfill the objectives. It is apparent if one considers the size of uncertainty or in general perturbations, a more securing controller is attained. Robust control methods, like H∞ and μ-synthesis, follow this line of design [1, 2].

Flight control is one of the applications mostly affected by perturbations. In this respect, many multivariable robust control techniques have been employed that an exhaustive compendium of them is found in [1]. In [3], H∞ and μ-synthesis approach have been studied for aircraft lateral movement. An analytic solution of nonlinear H∞ robust controller is proposed in [4] to control a vehicle with mass and moment inertia uncertainties. In [5], application of a robust sampled-data H∞-controller is demonstrated for a high-performance aircraft executing a high α stability-axis roll maneuver, and its performance is compared with that of the continuous-time and digital H∞-controller. Use of H∞ controller in noisy environments is the subject of study in [6]. The focus of [7] is the design and implementation of optimal controllers for a fixed-wing UAV lateral movement control. In [8], the automatic control of aircraft is considered in the lateral-directional plane during the landing approach phase. Generalized linear quadratic Gaussian and loop transfer recovery method is addressed in [9] . Comparative study of LQG/LTR with H∞ controllers has been reported in [10]. In [11], an approach to robust controller design that combines the recessive trait crossover genetic algorithm with the loop-shaping design procedure using H∞ synthesis has also been proposed.

In this study, the robust control methods including H∞, μ synthesis and the newly suggested μ-PID using intelligent optimization method are designed. The performances of the controllers in suppressing disturbances imposed on the systems are verified. The simulation result indicate that the robust methods all can accomplish the desired task, however, there is differences in how much they have been effective. In this respect, performance of lower sized μ-PID looks attractive and promising.

This paper is organized as follows. In section 2, the aircraft dynamic equation is presented. The controller designs are detailed in section 3. The comparative study of the methods performances are examined in section 4 and lastly conclusion comes in section 5.

2 SYSTEM DYNAMICAL MODEL

The nonlinear dynamic equation in compact form is given by,

$$\begin{aligned} &\dot{x} = f(x,u) \\ &x = [u, v, w, p, q, r, \varphi, \theta, \psi]^T, \\ &u = [\delta_e, \delta_a, \delta_r, \delta_T]^T \end{aligned} \tag{1}$$

where *u, v, w* are linear velocities along the body axes. p, q, r, ϕ, θ and ψ are roll, pitch and yaw rates and angles, respectively. The control vector *u* consists of elevator, aileron and rudder control surfaces plus propeller thrusting force. The expanded form of (1) is as bellow [12]

$$\dot{u} = rv - qw - g\sin\Theta + m^{-1}[f_x^{\alpha,V}(q,\delta_e) + f_T^V(\delta_T)]$$
$$\dot{v} = pw - ru + g\cos\Theta\sin\Phi + m^{-1}f_y^{\alpha,V}(\beta,\delta_a,\delta_e,p,r)$$
$$\dot{w} = qu - pv + g\cos\Theta\cos\Phi + m^{-1}f_z^{\alpha,V}(\beta,\delta_e,q)$$

$$\dot{p} = k^{-1}\left[c_1 rq + c_2 pq + T_l^{\alpha,V}(\beta,\delta_{ail},\delta_{rud},p,r)\right]$$
$$\dot{q} = I_{yy}^{-1}\left[(I_{zz} - I_{xx})pr - I_{xz}(p^2 - r^2) + T_m^{\alpha,V}(\delta_{elv},q)\right]$$
$$\dot{r} = k^{-1}\left[c_3 pq - c_2 rq + T_n^{\alpha,V}(\beta,\delta_{ail},\delta_{rud},p,r)\right] \qquad (2)$$

$$\dot{\phi} = p + \tan\theta(r\cos\phi + q\sin\phi)$$
$$\dot{\theta} = q\cos\phi - r\sin\phi$$
$$\dot{\psi} = \frac{r\cos\phi + q\sin\phi}{\cos\theta}$$
$$k = I_{xx}I_{zz} - I_{xz}^2, \quad c_1 = (I_{yy}I_{zz} - I_{zz}^2 - I_{xz}^2),$$
$$c_2 = (I_{xx} - I_{yy} + I_{zz})I_{xz}, \quad c_3 = (I_{xx}^2 - I_{yy}I_{xx} - I_{xz}^2)$$

where *m, I's, β, α* and *V* are the mass, rotational inertia along the related axes, sideslip angle, angle of attack and air speed, respectively. *f's* and *T's* are the forces and moments applied to the vehicle. The force and moments are nonlinear functions of aerodynamic parameters and time varying as the operating point of vehicle, i.e. α and *V,* change. The following auxiliary variables are expressed in terms of the state variables as below,

$$V = \sqrt{u^2 + v^2 + w^2} \qquad \alpha = tan^{-1}\left(w/u\right) \qquad \beta = sin^{-1}\left(v/V\right)$$

2.1 The Linearized system

Let's consider an aircraft with the specification depicted in Table 1 and the aerodynamic coefficients taken from [12].

TABLE 1. *Parameter of aircraft*

Parameter	value
m	20.500
Ix	9.496
Iy	55814
Iz	63100
Ixz	982
b (wing span)	30 (ft)
S (wing reference area)	300 (ft^2)
$\bar{c}$ (mean aerodynamic chord)	11.32 (ft)
$\bar{q}$ (dynamic pressure)	256.2139 (lb/ft)

The trim points of the aircraft nonlinear model (1) for a lateral maneuver in the horizontal plane is computed as below,

$[\delta_e, \delta_a, \delta_r, \delta_T]$=[-0.7588 0 0 0.1385]

[V α β φ θ p q r]=[17 2.11 0 0 2.11 0 0 0]

and the states involved are,

$$x = [\beta\ \varphi\ p\ r\ \delta_a\ \delta_r]^T$$

The presence of the control variables δ_a and δ_r, in the states is for the first order model of the actuators given by, 1/(s/20+1). Now, the input controls exciting the aileron and rudder actuators are, $u=[u_\phi \quad u_\beta]^T$ and the outputs of the MIMO system are $y=[\phi \quad \beta]^T$.

The linearized system equation around the given operating point is calculated as follows,

$$\dot{x}=Ax+Bu$$
$$y=Cx$$

$$A=\begin{bmatrix} -0.3019 & 0.06404 & 0.03529 & -0.9917 & 0.0002959 & 0.0008292 \\ 0 & 0 & 1 & 0.03573 & 0 & 0 \\ -28.86 & 0 & -3.618 & 0.06451 & -0.6809 & 0.1307 \\ 7.998 & 0 & -0.02552 & -0.4997 & -0.02989 & -0.06451 \\ 0 & 0 & 0 & 0 & -20 & 0 \\ 0 & 0 & 0 & 0 & 0 & -20 \end{bmatrix} \quad (3)$$

$$B=\begin{bmatrix} 0 & 0 & 0 & 0 & 1 & 0 \\ 0 & 0 & 0 & 0 & 0 & 1 \end{bmatrix}^{T}, \qquad C=\begin{bmatrix} 0 & 57.3 & 0 & 0 & 0 & 0 \\ 57.3 & 0 & 0 & 0 & 0 & 0 \end{bmatrix}$$

The roll angle versus u_ϕ is derived as given by,

$$G(s)=\frac{(-789.4s\hat{}2-668s-7380)}{s\hat{}5+24.62s\hat{}4+101.3s\hat{}3+274.9s\hat{}2+649.6s+10.61}$$

3 ROBUST DESIGNS

3.1 H_∞ Synthesis

Consider the uncertain system depicted in Fig. 1.

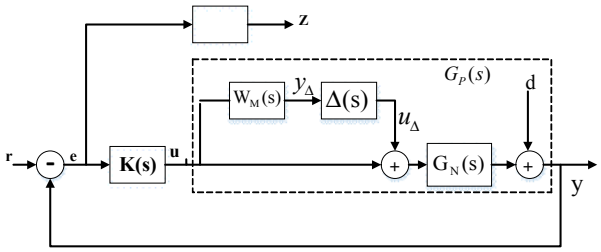

Fig. 1. The closed loop uncertain system [13].

The variables *r, d, u, y, e, z* are the reference vector, the disturbances, the control input, the measured output, the tracking error and the filtered tracking error, respectively. The Δ block represents the uncertainty in the system and G_n is the nominal system. The weighting function W_p is chosen as a high-gain low-pass filters to ensure that the outputs can be controlled accurately with good disturbance attenuation up to 10 rad/s.

By Ignoring the Δ block, P can be detailed as below [14],

$$\begin{cases} z=P_{11}(r-y)+P_{12}u \\ e=P_{21}(r-w)+P_{22}u \end{cases}, \qquad P(s)=\begin{bmatrix} P_{11}(s) & P_{12}(s) \\ P_{21}(s) & P_{22}(s) \end{bmatrix}$$

Upon application of the control signal u=Ke, z is obtained as follows,

$$z=F_L(P,K)w=\left[P_{11}+P_{12}K(I-P_{22}K)^{-1}P_{21}\right]w$$

The optimization process

$$\min_K \left\|L_L(P,K)\right\|_\infty < \gamma$$

is performed over the all controllers that stabilize the closed-loop system. Such optimization problem is called H_∞ standard problem.

Upon the selection of the design parameter,

$$W_p=\frac{0.95*(s+5.2)^2}{(s+0.001)*(s+9.3)}I_2 \quad (4)$$

and using MATLAB *hinfsyn* command, the two controllers are calculated where the one relating u_ϕ to ϕ is of order 7 which the order can be reduced to 5 without losing substantiate quantity in the frequency response, as given below,

$$K=\frac{u_\varphi}{e}=\frac{-3.84e5s^4-1.748e7s^3-2.163e8s^2-4.874e8s-8.326e6}{s^5+1409s^4+8.221e5s^3+2.706e8s^2+1.996e9s}$$

The obtained γ is 0.9535.

3.2 μ Synthesis

The block diagram depicted in Fig. 1, includes the nominal system G_N, the uncertainty model Δ, the controller K, the uncertainty weight function W_M and the performance weight function W_P. As it is mentioned, in the H_∞ design, no explicit use of uncertainty is applied and the Δ block is ignored. Differently, in μ synthesis the existing information about the uncertainty is enclosed in the design by the Δ block representing a stable random system with $\|\Delta\|_\infty<1$ and a fixed W_M which carries the pre knowledge about the distribution of the uncertainty in the various frequency bands. The performance measure is the structured singular value 'μ' used for both analyzing robustness in performance and synthesizing a robust controller [18].

Considering Fig.1, the following relationships can be established,

$$\begin{bmatrix} y_\Delta \\ z \end{bmatrix} = \begin{bmatrix} N_{11} & N_{12} \\ N_{21} & N_{22} \end{bmatrix} \begin{bmatrix} u_\Delta \\ d \end{bmatrix}$$

$$N_{11} = \frac{W_M GK}{1+GK} \qquad N_{12} = \frac{W_M K}{1+GK}$$

$$N_{21} = \frac{W_P G}{1+GK} \qquad N_{22} = \frac{W_p}{1+GK}$$

Based on the μ synthesis theory, robust stability is ensured if

$$\underset{\Delta}{\mu}(N_{11}) < 1$$

and robust performance is guaranteed by,

$$\underset{\Delta}{\mu}(N) < 1$$

The applied uncertainty is imposed by ±15% tolerance in the mass and ±15% perturbations in the aerodynamic forces and the moments. The bound of the uncertainty in the model is prescribed through the upper bound dotted curves in Fig. 2, which is given by,

$$W_M = \begin{bmatrix} \dfrac{4.0562(s^2+0.2291s+0.03129)}{(s+0.03602)(s+5.998)} & 0 \\ 0 & \dfrac{6.2362(s+0.03953)(s+6.753)}{(s+0.01687)(s+54.8)} \end{bmatrix} \tag{5}$$

and the performance requirement is enforced by (4) as it is done in the H_∞ design.

The controller is designed using *dksync* command. The result is a controller of order 17 with $\mu_{max}=0.961$. The controller size can be reduced to still large order 17 without degradation in the frequency response curve.

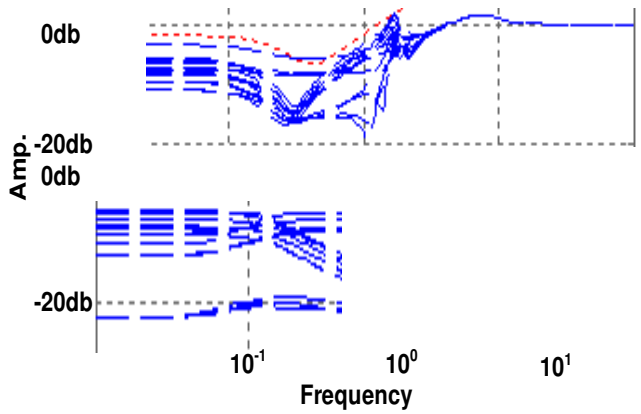

Fig. 2. The upper bound of the uncertainties applied.

4 MU-PID DESIGN

4.1 Particle Swarm Optimization

One of the approaches toward intelligent optimization is the particle swarm optimization (PSO) algorithm. The algorithm flies a set of particles over a search space to locate a global optimum, where a swarm of n particles communicate either directly or indirectly with one another [15]. PSO procedure is conducted through the following steps,

1. Pick n, the number of the particles in the population.
2. Initialize randomly the population
3. Evaluate fitness of each particle
4. Save the best particle as lbest
5. Update the global best, gbest
6. Modify velocities based on pbest and gbest, using (5)
7. Update the particle position,(6)
8. Terminate if the condition is met,
9. Go to step 2.

The basic concept of PSO lies in accelerating each particle toward the best position found by it so far (pbest) and the global best position (gbest) obtained so far by any particle, with a random weighted acceleration at each time step given by,

$$v_{t+1} = w \times v_t + c_1 \times rand\,(0,1) \times (pbest - x_1) + c_2 \times rand\,(0,1) \times (gbest - x_t)$$

where c_1 and c_2 are acceleration coefficients and w is the inertial weight. Then the next position of the particle is calculated by,

$$x_{t+1} = x_t + v_{t+1}$$

4.2 The performance index

For the μ-PID design, a new performance index containing the time domain and the frequency domain indices is proposed as defined below,

$$J(\theta) = w_1 P_{Mu} + w_2 M_p + w_3 t_r + w_4 t_s + w_5 \int_0^T te^2(t)dt$$

where $P_{MU,}$, M_p, t_r and t_s are peak mu bound, the step overshoot, rise time, settling time and integral time square of the tracking error, respectively. The weight factors must properly be set in order to surround the desired specification.

4.3 The μ-PID design process

The system is introduced by the following unstructured uncertainty input multiplicative model depicted in Fig. 1,

$$G(s) = G_N(s)(1 + W_M(s)\Delta(s))$$

Where $\Delta(s)$ is any stable and proper transfer function satisfying $\|\Delta\|_\infty<1$ and W_M to set the upper bound of the frequency response of the uncertain system as it is done by (5) in the μ-synthesis design. The performance weighting function $W_p(s)$ is chosen as the approximation of the inverse sensitivity function of an acceptable closed-loop system as it is done before by (4).

The PID controller is expressed in a matrix form as below,

$$u = [e \;\; \dot{e} \;\; \ddot{e}]\theta, \quad \theta = [k_P \;\; k_i \;\; k_d]^T, \quad e = \varphi_r - \varphi$$

and the weightings of,

$$w_1 = 150,\ w_2 = 3, w_3 = 1, w_4 = 1, w_5 = 100$$

are set.

Calculation of the performance index includes running μ synthesis *dksync* command for calculation of the peak mu bound M_{pu} and executing the closed loop step response for acquiring M_p, t_r, t_p and e. In case of arriving at an unstable system, J is penalized by a large positive number [24].

The PSO running parameters are:

- Population size =30.
- Acceleration constants $c_1 = 2$ and $c_2 = 2$.
- Maximum iteration is set to 1000.
- Inertia weight factor $w \in [0.4\ 0.9]$.
- The limit of change in velocity is set to maximum dynamic range of the variables on each dimension.

Upon execution of the program, the following PID controller parameters are obtained,

$$K_p = -0.2641, \quad K_I = -0.0132, \quad K_D = -0.0839$$

The plot of the μ band has been depicted in Fig. 3.

5 SIMULATION RESULTS

In this section, the performance of the designed controller: H_∞, μ synthesis and μ-PID in maintaining well-behaved roll response is examined.

The system is at stand still. At t=10 seconds a step is applied to the roll. Subsequently at 21th second, the system experience a pulse like disturbance of 2 seconds in duration. The system response has been depicted in Fig. 3. The μ synthesis and H∞ designs both show almost similar responses. The response of μ-PID, however, is smoother with less overshoot while preserving the settling time.

From viewpoint of the computation cost, H_∞ controller has the order of 4, the μ synthesis has order of 12 while the order of μ-PID is two. Therefore, it is concluded that μ-PID while enjoys the robustness of the μ synthesis method, has simple and low size structure. Keeping in mind that PID is the controller of choice in low maneuvering tasks, however, here it is designed in a way to provide better uncertainty accommodation.

A more illustrative picture projecting the differences in the controllers performances have been depicted in Fig. 4.

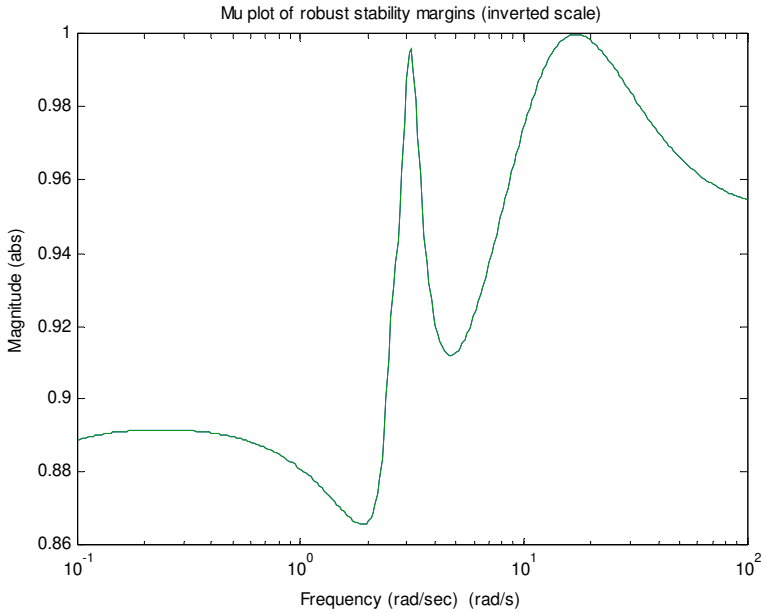

Fig. 3. The Mu bound for robust performance

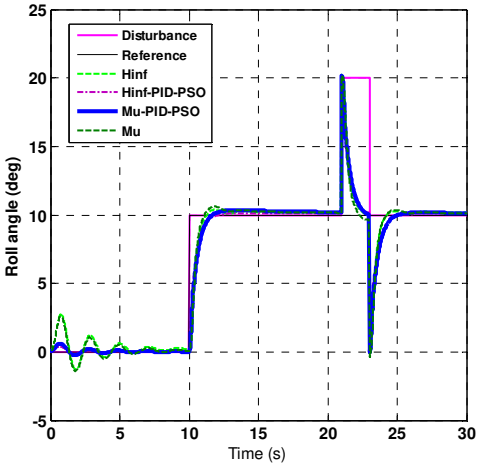

Fig. 4. The system step responses in facing the disturbance.

In another experiment, the impact of parameter uncertainties on the designed controllers is examined. In this respect, ±15% tolerance in the mass and ±15% perturbations in the aerodynamic forces and the moments are applied. Then, the aforementioned flight scenario is executed. The system performances in handling the uncertainties and the disturbance have been portrayed in Fig. 5 where coherent responses have been recorded.

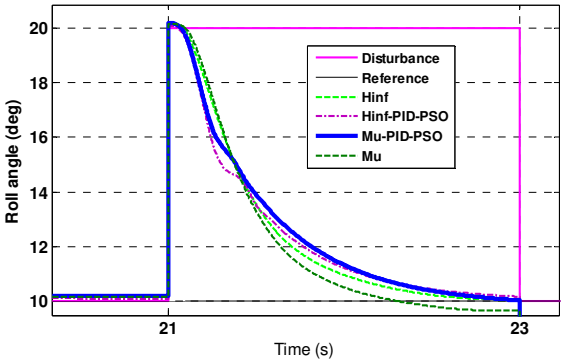

Fig. 5. A detailed graphs of the control systems step response behaviors.

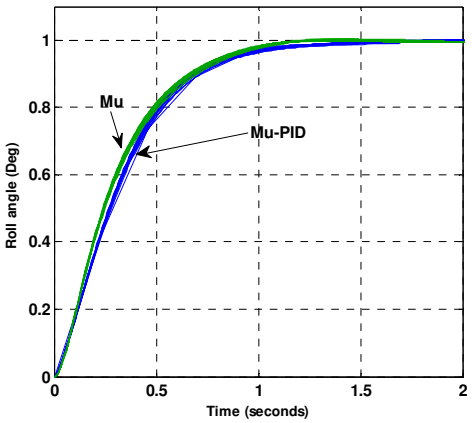

Fig. 6. The containments of the uncertainties by the robust lateral controllers.

6 CONCLSION

In this paper, the μ-PID controller design is suggested that combines the frequency domain merit of robust design and the time-domain performance objectives in a unified performance index. The nonlinear optimization problem is solved employing the intelligent PSO. The design is applied to the MIMO lateral flight control of an aircraft

along with the H_∞ and μ synthesis designs. The controllers suppress the effect of disturbances and tolerate the system uncertainties. However, lower sized μ-PID as a whole is exposed as more favorable.

REFERENCE

[1] J.-F. Magni, S. Bennani, and J. Terlouw. (1997, Robust flight control: a design challenge. *110*.

[2] W. C. Reigelsperger, K. D. Hammett, and S. S. Banda, "Robust control law design for lateral-directional modes of an F-16/MATV using μ-synthesis and dynamic inversion," *International Journal of Robust and Nonlinear Control,* vol. 7, pp. 777-795, 1997.

[3] R. Bréda, T. Lazar, R. Andoga, and L. Madarász, "Robust Controller in the Structure of Lateral Control of Maneuvering Aircraft," *Acta Polytechnica Hungarica,* vol. 10, pp. 101-124, 2013.

[4] C.-C. Kung, "Nonlinear H∞ robust control applied to F-16 aircraft with mass uncertainty using control surface inverse algorithm," *Journal of the Franklin Institute,* vol. 345, pp. 851-876, 2008.

[5] J.-S. Yee, J. L. Wang, and N. Sundararajan, "Robust sampled-data H∞-flight-controller design for high α stability-axis roll maneuver," *Control Engineering Practice,* vol. 8, pp. 735-747, 2000.

[6] J. López, R. Dormido, S. Dormido, and J. Gómez, "A Robust Controller for an UAV Flight Control System," *The Scientific World Journal,* vol. 2015, 2015.

[7] O. Arifianto and M. Farhood, "Optimal control of a small fixed-wing UAV about concatenated trajectories," *Control Engineering Practice,* vol. 40, pp. 113-132, 2015.

[8] R. Lungu and M. Lungu, "Automatic Control of Aircraft in Lateral-Directional Plane During Landing," *Asian Journal of Control,* 2015.

[9] H.-L. Tsai and J.-M. Lin, "Generalized linear quadratic gaussian and loop transfer recovery design of F-16 aircraft lateral control system," *lateral,* vol. 100, p. 6, 2007.

[10] J. Zarei, A. Montazeri, M. R. J. Motlagh, and J. Poshtan, "Design and comparison of LQG/LTR and H∞ controllers for a VSTOL flight control system," *Journal of the Franklin Institute,* vol. 344, pp. 577-594, 2007.

[11] A. El-Mahallawy, H. Yousef, M. El-Singaby, A. Madkour, and A. Youssef, "Robust flight control system design using H∞ loop-shaping and recessive trait crossover genetic algorithm," *Expert Systems with Applications,* vol. 38, pp. 169-174, 2011.

[12] F. R. Garza and E. A. Morelli, "A collection of nonlinear aircraft simulations in matlab," *NASA Langley Research Center, Technical Report NASA/TM,* vol. 212145, 2003.

[13] D.-W. Gu, P. Petkov, and M. M. Konstantinov, *Robust control design with MATLAB®*: Springer Science & Business Media, 2014.

[14] J. M. Maciejowski, "Multivariable feedback design," *Electronic Systems Engineering Series, Wokingham, England: Addison-Wesley,| c1989,* vol. 1, 1989.

[15] S. S. Aote, M. Raghuwanshi, and L. Malik, "A brief review on particle swarm optimization: limitations & future directions," *International Journal of Computer Science Engineering (IJCSE),* vol. 14, pp. 196-200, 2013.